

# Analytic and “frozen” QCD coupling constants up to NNLO from DIS data

A.V. Kotikov, V.G. Krivokhizhin, B.G. Shaikhatdenov  
 Joint Institute for Nuclear Research, Russia

June 16, 2018

## Abstract

Deep inelastic scattering data on the  $F_2$  structure function provided by the BCDMS, SLAC and NMC collaborations are analyzed in the non-singlet approximation with the analytic and “frozen” modifications of the strong coupling constant featuring no unphysical singularity (the Landau pole). Improvement of agreement between theory and experiment, with respect to the case of the standard perturbative definition of  $\alpha_s$  considered recently, is observed and the behavior of the higher twist terms in the next-to-next-to-leading-order is found to be confirming earlier studies on the subject.

*PACS*: 12.38 Aw, Bx, Qk

*Keywords*: Deep inelastic scattering; Nucleon structure functions; QCD coupling constant; NNLO level;  $1/Q^2$  power corrections.

## 1 Introduction

At present an accuracy of the data on the deep inelastic scattering (DIS) structure functions (SFs) makes it possible to study separately the  $Q^2$ -dependence of logarithmic QCD-inspired corrections and those of power-like (non-perturbative) nature (see for instance [1] and references therein).

This paper closely follows those devoted to the similar studies performed in [2, 3]. We analyze DIS SF  $F_2(x, Q^2)$  with SLAC, NMC and BCDMS experimental data involved [4]–[9]<sup>1</sup> up to the next-to-next-to-leading-order (NNLO) of massless perturbative QCD. This latter level of accuracy has become possible to ensure given the results obtained for both the  $\alpha_s^3(Q^2)$  corrections to the splitting functions (the anomalous dimensions of Wilson operators) [10] and the corresponding expressions of the complete three-loop coefficient functions for the structure functions  $F_2$  and  $F_L$  [11].

As in our previous papers the function  $F_2(x, Q^2)$  is represented as a sum of the leading twist  $F_2^{pQCD}(x, Q^2)$  and the twist four terms:

$$F_2(x, Q^2) = F_2^{pQCD}(x, Q^2) \left( 1 + \frac{\tilde{h}_4(x)}{Q^2} \right). \quad (1)$$

While analyzing experimental data various corrections must be taken into account. Here the nuclear effects, target mass corrections, heavy quark threshold corrections and higher twist (HT) terms are considered. For more details we refer to [3, 12].

---

<sup>1</sup>The BFP dataset, which was included in the analyses carried out in [2, 3], is excluded in this work since its influence here is negligible.

In the present work we study the effects of the popular infrared modifications of the strong coupling constant, such as the “frozen” [13] and the analytic [14] ones, and consider the change in the magnitudes of the twist four terms. These coupling constants are free of unphysical singularity in the infrared region of the scale  $\sim \Lambda$ .

As is known there are at least two ways of carrying out the QCD analysis over DIS data: the first one (see e.g. [15, 16]) deals with the Dokshitzer-Gribov-Lipatov-Altarelli-Parisi (DGLAP) integro-differential equations [17] and let the data be examined directly, whereas the second one involves the SF Mellin moments and permits performing an analysis in analytic form as opposed to the former option. In this work we adopt the analysis carried out over the moments of SF  $F_2^k(x, Q^2)$  defined as follows

$$M_n^{pQCD/twist2/\dots}(Q^2) = \int_0^1 x^{n-2} F_2^{pQCD/twist2/\dots}(x, Q^2) dx \quad (2)$$

and then reconstruct SF for each  $Q^2$  by using Jacobi polynomial expansion method [18]-[20] (for further details see [3, 12] and section 4).

The paper is organized as follows. In Sec. 2, we review theoretical aspects of the analysis. Sec. 3 contains infrared modifications of the strong coupling constant and the procedures to implement them into the representations for the SF Mellin moments. In Sec. 4, the SF fit method to follow is briefly described. The results obtained in two different schemes — the variable and fixed flavor number schemes — are given in Sec. 5. followed by the conclusions. In App. A, the results of the Fractional Analytic Perturbation Theory (FAPT) are adapted for the SF Mellin moments. App. B shows how an additional contribution to the structure function comes from the “analytization” of the coupling constant.

## 2 Theoretical aspects of the analysis

Here we describe the theoretical background of our analysis presented for the leading twist part. The coefficient  $\tilde{h}_4(x)$  of the twist-four correction is considered to be  $Q^2$ -independent and its  $x$  shape is determined from the fits to the DIS structure functions. For a bit detailed account see also [3].

The leading twist DIS SF can be represented as a sum of two terms:  $F_2^{twist2}(x, Q^2) = F_2^{NS}(x, Q^2) + F_2^S(x, Q^2)$ , the nonsinglet (NS) and singlet (S) parts. At this point let’s introduce parton distribution functions (PDFs), the gluon distribution function  $f_G(x, Q^2)$  and the singlet and nonsinglet quark distribution functions  $\mathbf{f}_S(x, Q^2)$  and  $\mathbf{f}_{NS}(x, Q^2)$ <sup>2</sup>:

$$\begin{aligned} \mathbf{f}_S(x, Q^2) &\equiv \sum_q^f \mathbf{f}_q(x, Q^2) = V(x, Q^2) + S(x, Q^2), \\ \mathbf{f}_{NS}(x, Q^2) &= \mathbf{u}_v(x, Q^2) - \mathbf{d}_v(x, Q^2), \end{aligned}$$

where  $f$  is the number of quark flavors (**u**p, **d**own, **s**trange, . . .),  $V(x, Q^2) = \mathbf{u}_v(x, Q^2) + \mathbf{d}_v(x, Q^2)$  is the distribution of valence quarks and  $S(x, Q^2)$  is a sum of sea parton distributions set equal to each other.

As is known, at large values of  $x$  ( $x \geq 0.25$ ) the contribution of sea parton distributions  $S(x, Q^2)$  is negligible and, therefore,  $\mathbf{f}_S(x, Q^2)$  and  $\mathbf{f}_{NS}(x, Q^2)$  (and correspondingly  $F_2^{NS}(x, Q^2)$  and  $F_2^S(x, Q^2)$ ) appear to have similar  $Q^2$ -dependence.

In the present paper we restrict analysis to the large  $x$  region. Consequently, the analysis is dubbed the “nonsinglet” one (simply signaling the absence of gluons) but actually the data on the entire SF  $F_2(x, Q^2)$  will be considered.

---

<sup>2</sup>Unlike the standard case, here PDFs are multiplied by  $x$ .

There is a direct relation between SF moments (2) and those of PDFs

$$\mathbf{f}_{NS}(n, Q^2) = \int_0^1 dx x^{n-2} \mathbf{f}_{NS}(x, Q^2).$$

For example, in the nonsinglet case it is found to be [21]:

$$M_n^{NS}(Q^2) = R_{NS}(f) \cdot C_{NS}^{twist2}(n, a_s(Q^2)) \cdot \mathbf{f}_{NS}(n, Q^2), \quad (3)$$

with  $a_s(Q^2) = \alpha_s(Q^2)/(4\pi)$  and  $C_{NS}^{twist2}(n, a_s(Q^2))$  being the Wilson coefficient functions. The constant  $R_{NS}(f)$  depends on weak and electromagnetic charges and is fixed to be one sixth for  $f = 4$  [21].

Considerations of such issues as the PDF normalization, target mass (TMC) and higher twist corrections (HTCs), as well as nuclear effects, remain essentially the same as in our previous work [3] so we refer to it for further details, though quoting some salient points.

A starting point of the evolution is taken at relatively large values  $Q_0^2$ . There is a number of reasons behind that choice, e.g., fewer heavy quark thresholds have to be crossed to reach a normalization point, a perturbative approach must be applicable at the value of  $Q_0^2$ . Besides, impact of higher order corrections derived from PDF normalization conditions is the more negligible the higher normalization point is.

The moments  $\mathbf{f}_{NS}(n, Q^2)$  at some  $Q_0^2$  is a theoretical input to the analysis which is fixed as follows. In the fits of data with the cut  $x \geq 0.25$  imposed only the nonsinglet parton density is worked with and the following parametrization at the normalization point is used (see, for example, [22, 23]):

$$\begin{aligned} \mathbf{f}_{NS}(n, Q_0^2) &= \int_0^1 dx x^{n-2} \tilde{\mathbf{f}}_{NS}(x, Q_0^2), \\ \tilde{\mathbf{f}}_{NS}(x, Q_0^2) &= A_{NS}(Q_0^2)(1-x)^{b_{NS}(Q_0^2)}(1+d_{NS}(Q_0^2)x), \end{aligned} \quad (4)$$

where  $A_{NS}(Q_0^2)$ ,  $b_{NS}(Q_0^2)$  and  $d_{NS}(Q_0^2)$  are some coefficients<sup>3</sup>.

## 2.1 Strong coupling constant

The strong coupling constant is determined from the renormalization group equation to an accuracy of  $\mathcal{O}(10^{-5})$  (which is enough for our purposes, also we checked that for higher precision the results get no much better). At NLO level the latter is given by

$$\frac{1}{a_s^{(0)}(Q^2)} - \frac{1}{a_s^{(0)}(M_Z^2)} = \beta_0 \ln \left( \frac{Q^2}{M_Z^2} \right), \quad (5)$$

$$\frac{1}{a_s^{(1)}(Q^2)} - \frac{1}{a_s^{(1)}(M_Z^2)} + b_1 \ln \left[ \frac{a_s^{(1)}(Q^2)}{a_s^{(1)}(M_Z^2)} \frac{(1+b_1 a_s^{(1)}(M_Z^2))}{(1+b_1 a_s^{(1)}(Q^2))} \right] = \beta_0 \ln \left( \frac{Q^2}{M_Z^2} \right), \quad (6)$$

where hereinafter the strong coupling constant at the leading order (LO), next-to-leading order (NLO) and NNLO levels of approximation will be denoted by  $a_s^{(i)}(Q^2)$  with  $i = 0, 1$  and 2, respectively. Furthermore, we will designate  $a_s^{(2)}(Q^2)$  as  $a_s(Q^2)$  to simplify notation, as it is the NNLO approximation that is of special interest in the present analysis.

At NNLO level the strong coupling constant is derived from the following equation:

$$\begin{aligned} \frac{1}{a_s(Q^2)} - \frac{1}{a_s(M_Z^2)} + b_1 \ln \left[ \frac{a_s(Q^2)}{a_s(M_Z^2)} \sqrt{\frac{1+b_1 a_s(M_Z^2) + b_2 a_s^2(M_Z^2)}{1+b_1 a_s(Q^2) + b_2 a_s^2(Q^2)}} \right] \\ + \left( b_2 - \frac{b_1^2}{2} \right) \cdot (I(a_s(Q^2)) - I(a_s(M_Z^2))) = \beta_0 \ln \left( \frac{Q^2}{M_Z^2} \right). \end{aligned} \quad (7)$$

<sup>3</sup>Here we do not consider the term  $\sim x^{a_{NS}(Q_0^2)}$  in the normalization of  $\tilde{\mathbf{f}}_{NS}(x, Q_0^2)$ , because of the cut  $x \geq 0.25$ .

The expression for  $I$  looks like

$$I(a_s(Q^2)) = \begin{cases} \frac{2}{\sqrt{\Delta}} \arctan \frac{b_1 + 2b_2 a_s(Q^2)}{\sqrt{\Delta}} & \text{for } f = 3, 4, 5; \Delta > 0, \\ \frac{1}{\sqrt{-\Delta}} \ln \left[ \frac{b_1 + 2b_2 a_s(Q^2) - \sqrt{-\Delta}}{b_1 + 2b_2 a_s(Q^2) + \sqrt{-\Delta}} \right] & \text{for } f = 6; \quad \Delta < 0, \end{cases}$$

where  $\Delta = 4b_2 - b_1^2$  and  $b_i = \beta_i/\beta_0$  are read off from the QCD  $\beta$ -function:

$$\beta(a_s) = -\beta_0 a_s^2 - \beta_1 a_s^3 - \beta_2 a_s^4 + \dots \quad (8)$$

## 2.2 $Q^2$ -dependence of SF moments

The coefficient functions  $C_{NS}^{twist2}(n, a_s(Q^2))$  are further expressed through the functions  $B_{NS}^{(i)}(n)$  ( $i = 1, 2$ ), which are known exactly [11, 21]<sup>4</sup>

$$C_{NS}^{twist2}(n, a_s(Q^2)) = 1 + a_s B_{NS}^{(1)}(n) + a_s^2 B_{NS}^{(2)}(n) + \mathcal{O}(a_s^3). \quad (9)$$

The  $Q^2$ -evolution of the PDF moments can be calculated within a framework of perturbative QCD (see e.g. [21, 27]) to yield:

$$\frac{\mathbf{f}_{NS}(n, Q^2)}{\mathbf{f}_{NS}(n, Q_0^2)} = \left[ \frac{a_s(Q^2)}{a_s(Q_0^2)} \right]^{\frac{\gamma_{NS}^{(0)}(n)}{2\beta_0}} \frac{h^{NS}(n, Q^2)}{\bar{h}^{NS}(n, Q_0^2)}, \quad (10)$$

$$h^{NS}(n, Q^2) = 1 + a_s(Q^2) Z_{NS}^{(1)}(n) + a_s^2(Q^2) Z_{NS}^{(2)}(n) + \mathcal{O}(a_s^3(Q^2)) \quad (11)$$

and [28]

$$\begin{aligned} Z_{NS}^{(1)}(n) &= \frac{1}{2\beta_0} \left[ \gamma_{NS}^{(1)}(n) - \gamma_{NS}^{(0)}(n) b_1 \right], \\ Z_{NS}^{(2)}(n) &= \frac{1}{4\beta_0} \left[ \gamma_{NS}^{(2)}(n) - \gamma_{NS}^{(1)}(n) b_1 + \gamma_{NS}^{(0)}(n) (b_1^2 - b_2) \right] + \frac{1}{2} \left( Z_{NS}^{(1)}(n) \right)^2. \end{aligned} \quad (12)$$

Here  $\gamma_{NS}^{(k)}(n)$  are the factors before  $a_s$  in the expansion with respect to the latter of the anomalous dimensions  $\gamma_{NS}(n, a_s)$  (taken in the exact form from [10]).

## 3 Infrared modifications of the strong coupling constant

Here, we investigate the potential of modifying the strong-coupling constant in the infrared region with the purpose of illuminating the problem related to the Landau singularity in QCD.

Specifically, we consider two modifications, which effectively increase the argument of the strong-coupling constant at small  $Q^2$  values, in accordance with [29].

In the first case, which is more phenomenological, we introduce freezing of the strong-coupling constant by changing its argument as  $Q^2 \rightarrow Q^2 + M_\rho^2$ , where  $M_\rho$  is the rho-meson mass [13] (see also [30, 24] and references therein). Thus, in the formulas of the previous section the following replacement is to be done:

$$a_s^{(i)}(Q^2) \rightarrow a_s^{(i),\text{fr}}(Q^2) = a_s^{(i)}(Q^2 + M_\rho^2) \quad (i = 0, 1, 2). \quad (13)$$

<sup>4</sup>For the odd  $n$  values, the coefficients  $B_{NS}^{(i)}(n)$  and  $Z_{NS}^{(i)}(n)$  ( $i = 1, 2$ ) can be obtained by using the analytic continuation [20, 25, 26].

A second possibility is based on the idea proposed by Shirkov and Solovtsov [14, 31] (see also recent reviews [32] and references therein) regarding the analyticity of the strong coupling constant in the complex  $Q^2$ -plane in the form of the Källén-Lehmann spectral representation. This approach leads effectively to additional power  $Q^2$ -dependence for the DIS structure functions (see Eq. (B2)).

### 3.1 Naive case

This modification is in a sense quite similar to the freezing procedure given above (13), i.e. the one- and two-loop coupling constants  $\alpha_s^{(0)}(Q^2)$  and  $\alpha_s^{(1)}(Q^2)$  appearing in the formulas of Subsec. 2.1 are to be replaced as follows:

$$a_s^{(0)}(Q^2) \rightarrow a_s^{(0),\text{an}}(Q^2) = a_s^{(0)}(Q^2) - \frac{1}{\beta_0} \frac{\Lambda_{(0)}^2}{Q^2 - \Lambda_{(0)}^2}, \quad (14)$$

$$a_s^{(1)}(Q^2) \rightarrow a_s^{(1),\text{an}}(Q^2) = a_s^{(1)}(Q^2) - \frac{1}{2\beta_0} \frac{\Lambda_{(1)}^2}{Q^2 - \Lambda_{(1)}^2} + \dots, \quad (15)$$

where the ellipsis stands for cut terms which give negligible contributions in our analysis.

At the one-loop level, the expression for the analytic coupling constant (14) is very simple. However, at higher-loop levels, it has a rather cumbersome structure (see a recent paper [33] and discussions therein). Therefore, it seems to be simpler to use some proper approximations so as to be able to carry out a numeric analysis.

Considering the study [31], in the NLO case the difference between analytic and standard coupling constants can be represented in the form given in (15), which is similar to the LO one with the additional coefficient equal to 1/2. Note that numerically this NLO term is quite analogous to the LO one, since  $\Lambda_{(0)} \ll \Lambda_{(1)}$  (see, for example, [34]).

Following the logic expounded in [24], where it was shown that at the NNLO level the effective LO  $\Lambda_{(0)}^{eff}$  can approximately be taken to be

$$\Lambda_{(0)}^{eff} = (2\pi^2)^{\frac{-\beta_1}{2\beta_0^2}} \Lambda \sim \frac{1}{2} \Lambda, \quad (16)$$

we can apply a simple analytic form in the NNLO as follows <sup>5</sup>

$$a_s(Q^2) \rightarrow a_s^{\text{an}}(Q^2) = a_s(Q^2) - \frac{1}{4\beta_0} \frac{\Lambda^2}{Q^2 - \Lambda^2} + \dots. \quad (17)$$

Thus, we propose to use this last expression in the NNLO approximation.

Since in our analyses Eqs. (6) and (7) were used to derive the strong coupling constant, the additional terms in (14), (15) and (17) can be represented as the functions of the ratio  $\Lambda_{(i)}^2/Q^2$ , which should be obtained from the corresponding equations

$$\frac{1}{a_s^{(0)}(Q^2)} = \beta_0 \ln \left( \frac{Q^2}{\Lambda_{(0)}^2} \right), \quad (18)$$

$$\frac{1}{a_s^{(1)}(Q^2)} + b_1 \ln \left[ \frac{\beta_0 a_s^{(1)}(Q^2)}{1 + b_1 a_s^{(1)}(Q^2)} \right] = \beta_0 \ln \left( \frac{Q^2}{\Lambda_{(1)}^2} \right), \quad (19)$$

$$\frac{1}{a_s(Q^2)} + b_1 \ln \left[ \frac{\beta_0 a_s(Q^2)}{\sqrt{1 + b_1 a_s(Q^2) + b_2 a_s^2(Q^2)}} \right] \quad (20)$$

---

<sup>5</sup>To have the poles in (15) and (17) exactly cancelled by those in the perturbative expansions of QCD coupling (see, for example, [2]), we keep  $Q^2 - \Lambda_{(i)}^2$  ( $i = 0, 1, 2$ ) in the denominators of the additional terms (i.e. in the last terms of (15) and (17)) and, therefore, above LO we will have additional terms coinciding with those in the LO case (with the corresponding replacements  $\Lambda_0 \rightarrow \Lambda_1$  and  $\Lambda_0 \rightarrow \Lambda$ ) multiplied by the additional factor  $1/(2i)$ .

$$+ \left( b_2 - \frac{b_1^2}{2} \right) I(a_s(Q^2)) = \beta_0 \ln \left( \frac{Q^2}{\Lambda^2} \right).$$

In a sense, the replacement quoted in (14), (15) and (17) is a naive way of doing “analytization”; we apply the latter procedure to the coupling constant itself without considering its actual function given by Eqs. (3), (9) and (10). Nonetheless, this procedure has already been successfully applied in [30, 35] for analyzing the DIS structure functions at small  $x$  values. With this motivation we would like to investigate its effect in the present study as well. Here it will be referred to as a procedure of the *naive “analytization”*.

### 3.2 Transition to the canonical form

To accomplish the procedure of “analytization” more accurately<sup>6</sup>, it is convenient for the moment  $M_n^{NS}(Q^2)$  given in Eq. (3) to be represented in the following form (see [36] and discussions therein)

$$M_n^{NS}(Q^2) = R_{NS}(f) \cdot \left[ \mu_n^{NS}(Q^2, Q_0^2) \right]^{\frac{\gamma_{NS}^{(0)}(n)}{2\beta_0}} \quad (21)$$

where the new “moment”  $\mu_n^{NS}(Q^2)$  is set to be

$$\begin{aligned} \mu_n^{NS}(Q^2, Q_0^2) &= \left( 1 + a_s(Q^2)b_{NS}^{(1)}(n) + a_s^2(Q^2)b_{NS}^{(2)}(n) \right) \\ &\times \frac{a_s(Q^2)}{a_s(Q_0^2)} \cdot \frac{1 + a_s(Q^2)z_{NS}^{(1)}(n) + a_s^2(Q^2)z_{NS}^{(2)}(n)}{1 + a_s(Q_0^2)z_{NS}^{(1)}(n) + a_s^2(Q_0^2)z_{NS}^{(2)}(n)} \\ &= \frac{a_s(Q^2)}{a_s(Q_0^2)} \cdot \frac{1 + a_s(Q^2)\tilde{B}^{(1)}(n) + a_s^2(Q^2)\tilde{B}_{NS}^{(2)}(n)}{1 + a_s(Q_0^2)z_{NS}^{(1)}(n) + a_s^2(Q_0^2)z_{NS}^{(2)}(n)} \end{aligned} \quad (22)$$

where

$$\begin{aligned} \tilde{B}^{(1)}(n) &= b_{NS}^{(1)}(n) + z_{NS}^{(1)}(n), \\ \tilde{B}^{(2)}(n) &= b_{NS}^{(2)}(n) + z_{NS}^{(2)}(n) + b_{NS}^{(1)}(n)z_{NS}^{(1)}(n) \end{aligned} \quad (23)$$

and

$$\begin{aligned} z_{NS}^{(1)}(n) &= \frac{\gamma_{NS}^{(1)}(n)}{\gamma_{NS}^{(0)}(n)} - b_1, \quad b_{NS}^{(1)}(n) = \frac{2\beta_0}{\gamma_{NS}^{(0)}(n)} B_{NS}^{(1)}(n), \\ b_{NS}^{(2)}(n) &= \frac{2\beta_0}{\gamma_{NS}^{(0)}(n)} B_{NS}^{(2)}(n) - \frac{1}{2} \left( \frac{\gamma_{NS}^{(0)}(n)}{2\beta_0} - 1 \right) \left( b_{NS}^{(1)}(n) \right)^2, \\ z_{NS}^{(2)}(n) &= \frac{1}{2} \left[ \frac{\gamma_{NS}^{(2)}(n)}{\gamma_{NS}^{(0)}(n)} - b_2 + b_1 \left( b_1 - \frac{\gamma_{NS}^{(1)}(n)}{\gamma_{NS}^{(0)}(n)} \right) \right] + \frac{1}{2} \left( z_{NS}^{(1)}(n) \right)^2. \end{aligned} \quad (24)$$

The procedure (21) has already been used in [22, 37], where the Grunberg’s effective method [38] has been incorporated into the analyses of DIS structure functions.

Now, the “moment”  $\mu_n^{NS}(Q^2)$  has the form close to that obtained for the sum rule, because it begins with  $a_s(Q^2)$  rather than a constant. Consequently, the form gets closer to that in the difference between the QCD sum rule and its Parton Model value. Following [24], the analytical version of Eq. (21) can be obtained by replacing Eq. (22) for the following ones:

$$\begin{aligned} \mu_{(0),n}^{NS}(Q^2, Q_0^2) &= \frac{A_1^{(1)}(Q^2)}{A_1^{(1)}(Q_0^2)}, \quad \mu_{(1),n}^{NS}(Q^2, Q_0^2) = \frac{A_1^{(2)}(Q^2) + A_2^{(2)}(Q^2)\tilde{B}^{(1)}(n)}{A_1^{(2)}(Q_0^2) + A_2^{(2)}(Q_0^2)z_{NS}^{(1)}(n)}, \\ \mu_n^{NS}(Q^2, Q_0^2) &= \frac{A_1^{(3)}(Q^2) + A_2^{(3)}(Q^2)\tilde{B}^{(1)}(n) + A_3^{(3)}(Q^2)\tilde{B}_{NS}^{(2)}(n)}{A_1^{(3)}(Q_0^2) + A_2^{(3)}(Q_0^2)z_{NS}^{(1)}(n) + A_3^{(3)}(Q_0^2)z_{NS}^{(2)}(n)}, \end{aligned} \quad (25)$$

<sup>6</sup>We will call this case an ordinary *analytic perturbation theory (APT)*.

where  $A_m^{(i)}$  is the ‘‘analytized’’  $m$ -th power of  $i$ -loop QCD coupling [14]. Thus, in the APT case the procedure features more complicated functions rather than just the powers of some coupling constant. In the one-loop case the Euclidean functions of analytic perturbation theory (APT)  $A_k^{(1)}(Q^2)$  are found to be [31]

$$\begin{aligned} A_1^{(1)}(Q^2) &= \frac{1}{\beta_0} \left[ \frac{1}{L_{(0)}} - \frac{\Lambda_{(0)}^2}{Q^2 - \Lambda_{(0)}^2} \right], & A_{k+1}^{(1)} &= -\frac{1}{k\beta_0} \frac{dA_k^{(1)}}{dL_{(0)}}, \\ A_2^{(1)}(Q^2) &= \frac{1}{\beta_0^2} \left[ \frac{1}{(L_{(0)})^2} - \frac{\Lambda_{(0)}^2 Q^2}{(Q^2 - \Lambda_{(0)}^2)^2} \right], \\ A_3^{(1)}(Q^2) &= \frac{1}{\beta_0^3} \left[ \frac{1}{(L_{(0)})^3} - \frac{\Lambda_{(0)}^2 Q^2 (Q^2 + \Lambda_{(0)}^2)}{2(Q^2 - \Lambda_{(0)}^2)^3} \right], \end{aligned} \quad (26)$$

where  $L_{(0)} = \ln(Q^2/(\Lambda_{(0)}^2)^2)$ , while beyond the LO approximation [31, 24] the transform from standard perturbation theory to the APT is slightly modified to assume the following form:

$$\begin{aligned} a_s^{(i)}(Q^2) \rightarrow A_1^{(i+1)}(Q^2) &= a_s^{(i)}(Q^2) - \frac{1}{2i\beta_0} \frac{\Lambda_{(i)}^2}{Q^2 - \Lambda_{(i)}^2}, \quad (i = 1, 2) \\ (a_s^{(i)}(Q^2))^2 \rightarrow A_2^{(i+1)}(Q^2) &= (a_s^{(i)}(Q^2))^2 - \frac{1}{2i\beta_0^2} \frac{\Lambda_{(i)}^2 Q^2}{(Q^2 - \Lambda_{(i)}^2)^2}, \\ (a_s^{(i)}(Q^2))^3 \rightarrow A_3^{(i+1)}(Q^2) &= (a_s^{(i)}(Q^2))^3 - \frac{1}{2i\beta_0^3} \frac{\Lambda_{(i)}^2 Q^2 (Q^2 + \Lambda_{(i)}^2)}{2(Q^2 - \Lambda_{(i)}^2)^3}, \end{aligned} \quad (27)$$

where the NLO and NNLO results (for  $i = 1$  and  $2$ ) are only some approximations.

To clear up with the meaning of all these formulas, we would like to note one more time that in the expressions for  $A_m^{(i)}(Q^2)$  the lower subscript stands for the power of the coupling constant, while the upper one is related with the order of the approximation considered. Therefore, if the  $\alpha_s$ -expansion of some variable starts with the first power, as is the case at hand, then the power of the last term of the expansion coincides with the order of the approximation, i.e. for the last term upper and lower subscripts coincide.

### 3.3 Fractional analytic perturbation theory

Recently, in a series of papers [39], the analytic continuation (26) has been extended to the noninteger powers of LO  $L_{(0)}^{-1}$ . In the one-loop case, this so-called fractional APT (FAPT) gives:

$$\frac{1}{L_{(0)}^\nu} \rightarrow \frac{1}{L_{(0)}^\nu} - \frac{\text{Li}_{1-\nu}(e^{-L_{(0)}})}{\Gamma(\nu)}, \quad (28)$$

where

$$\text{Li}_\nu(z) = \sum_{m=1}^{\infty} \frac{z^m}{m^\nu} \quad (29)$$

is actually the polylogarithm function.<sup>7</sup>

It is clearly seen that by virtue of

$$\text{Li}_0(z) = \frac{z}{1-z}, \quad \text{Li}_{-N}(z) = \left( z \frac{d}{dz} \right)^N \frac{z}{1-z} = \left( z \frac{d}{dz} \right)^N \frac{1}{1-z}, \quad (30)$$

all the equations quoted in (26) can be shown to be well reproduced.

<sup>7</sup>In [39] it was called the Lerch transcendent function.

Since the product of  $\Gamma$ -functions satisfy

$$\Gamma(\nu)\Gamma(1-\nu) = \frac{\pi}{\sin(\pi\nu)},$$

it is easy to obtain the following representation (see Appendix A):

$$\frac{\text{Li}_{1-\nu}(z)}{\Gamma(\nu)} = \frac{z}{\Gamma(\nu)\Gamma(1-\nu)} \int_0^1 \frac{d\xi}{1-z\xi} \ln^{-\nu}\left(\frac{1}{\xi}\right) = \frac{z \sin(\pi\nu)}{\pi} \int_0^1 \frac{d\xi}{1-z\xi} \ln^{-\nu}\left(\frac{1}{\xi}\right), \quad (31)$$

that holds for  $\Re(1-\nu) > 0$  and  $\Re(\nu) > 0$  (in the case at hand these boil down to  $0 < \nu < 1$ ).

Then, following the previous section let's recast Eq.(28) in the following fashion:

$$\left(a_s^{(0)}(Q^2)\right)^\nu \rightarrow A_\nu^{(1)}(Q^2) = \left(a_s^{(0)}(Q^2)\right)^\nu - \frac{\text{Li}_{1-\nu}\left(\Lambda_{(0)}^2/Q^2\right)}{\beta_0^\nu \Gamma(\nu)}, \quad (32)$$

which reproduces the equations in (26) with  $\nu = 1, 2$  and  $3$ , in order.

Above LO, using quite the same arguments as in the previous subsection we have similarly

$$\left(a_s^{(i)}(Q^2)\right)^\nu \rightarrow A_\nu^{(i+1)}(Q^2) = \left(a_s^{(i)}(Q^2)\right)^\nu - \frac{\text{Li}_{1-\nu}\left(\Lambda_{(i)}^2/Q^2\right)}{2i\beta_0^i \Gamma(\nu)}, \quad (i = 1, 2), \quad (33)$$

which in turn reproduces a set of equations quoted in (27) for  $\nu = 1, 2$  and  $3$ , respectively.

Note that the Mellin moments (10) used in this case, contain  $\nu = \gamma_{NS}^{(0)}(n)/(2\beta_0) + i$  with  $i = 0$  in the LO,  $i = 0, 1$  — NLO, and  $i = 0, 1, 2$  — NNLO approximations. The argument of the polylogarithm function  $\Lambda_{(i)}^2/Q^2$  found in Eqs. (32) and (33) can be expressed through the strong coupling constant as was explained in Subsec. 3.1 (see Eqs. (18)–(20)). Therefore, the power  $\nu$  lies within the range  $0 < \nu < 4$ , because  $0 < \gamma_{NS}^{(0)}(n)/(2\beta_0) < 2$  for  $2 < n < 10$  used in the analyses. The integral representation given in Eq. (31) is correct only for  $0 < \nu < 1$ , hence the need to extend it to higher values of  $\nu$ . Omitting details of this latter extension<sup>8</sup> we have

$$\frac{\text{Li}_{1-N-\delta}(z)}{\Gamma(N+\delta)} = \left(z \frac{d}{dz}\right)^N \left[ \frac{z}{\Gamma(N+\delta)\Gamma(1-\delta)} \int_0^1 \frac{d\xi}{1-z\xi} \ln^{-\delta}\left(\frac{1}{\xi}\right) \right] \quad (0 < \delta < 1). \quad (34)$$

To cover an entire range  $0 < \nu < 4$ , we should consider  $N = 0, 1, 2$  and  $3$ . For  $N = 0$ , Eq. (31) with the corresponding replacement  $\nu \rightarrow \delta$  can be used. For  $N > 0$ , it is straightforward to obtain

$$\begin{aligned} \left(z \frac{d}{dz}\right) \frac{z}{1-z\xi} &= \frac{z}{(1-z\xi)^2}, & \left(z \frac{d}{dz}\right)^2 \frac{z}{1-z\xi} &= \frac{z(1+z\xi)}{(1-z\xi)^3}, \\ \left(z \frac{d}{dz}\right)^3 \frac{z}{1-z\xi} &= \frac{z(1+4z\xi+z^2\xi^2)}{(1-z\xi)^4} \end{aligned} \quad (35)$$

and make use of the following formulas valid for  $0 < \delta < 1$ :

$$\frac{\text{Li}_{-\delta}(z)}{\Gamma(1+\delta)} = \frac{z}{\Gamma(1+\delta)\Gamma(1-\delta)} \int_0^1 \frac{d\xi \ln^{-\delta}(1/\xi)}{(1-z\xi)^2}, \quad (36)$$

$$\frac{\text{Li}_{-1-\delta}(z)}{\Gamma(2+\delta)} = \frac{z}{\Gamma(2+\delta)\Gamma(1-\delta)} \int_0^1 \frac{d\xi \ln^{-\delta}(1/\xi)}{(1-z\xi)^3} [1+z\xi], \quad (37)$$

$$\frac{\text{Li}_{-2-\delta}(z)}{\Gamma(3+\delta)} = \frac{z}{\Gamma(3+\delta)\Gamma(1-\delta)} \int_0^1 \frac{d\xi \ln^{-\delta}(1/\xi)}{(1-z\xi)^4} [1+4z\xi+z^2\xi^2], \quad (38)$$

<sup>8</sup>This is done in Appendix A (see Eqs. (A3) and (A4)) for  $\nu = N + \delta$ , where  $N = 1, 2, 3$ .

i.e. Eqs. (36), (37) and (38) can be used within the ranges  $1 < \nu < 2$ ,  $2 < \nu < 3$  and  $3 < \nu < 4$ , respectively.

Note that for  $\bar{\delta} \equiv 1 - \delta$  we have  $\delta = 1 - \bar{\delta}$ ,  $1 + \delta = 2 - \bar{\delta}$  and  $2 + \delta = 3 - \bar{\delta}$ . Hence, Eqs. (36), (37) and (38) can also be used in the ranges  $0 < \nu < 1$ ,  $1 < \nu < 2$  and  $2 < \nu < 3$ , respectively, if we replace  $\delta \rightarrow -\bar{\delta}$  in their r.h.s. It is a strong cross-check of the formulas presented in (36), (37) and (38).

## 4 A fitting procedure

A numeric procedure of data fitting is described in the previous papers [2, 3]. Here we just recall some aspects of the so-called polynomial expansion method. The latter was first proposed in [40] and further developed in [41]. In these papers the method was based on the Bernstein polynomials and subsequently used to analyze data at NLO [42, 25] and NNLO level [43, 44]. The Jacobi polynomials for that purpose were first proposed and then subsequently developed in [18, 19, 20] and used in [22, 28, 23, 44, 37]

With the QCD expressions for the Mellin moments  $M_n^k(Q^2)$  (k=pQCD,twist2, ...) analytically calculated according to the formula in (2), the SF  $F_2^k(x, Q^2)$  is reconstructed by using the Jacobi polynomial expansion method:

$$F_2^k(x, Q^2) = x^a(1-x)^b \sum_{n=0}^{N_{max}} \Theta_n^{a,b}(x) \sum_{j=0}^n c_j^{(n)}(\alpha, \beta) M_{j+2}^k(Q^2),$$

where  $\Theta_n^{a,b}$  are the Jacobi polynomials and  $a, b$  are the parameters to be fit. A condition put on the latter is the requirement of the error minimization while reconstructing the structure functions.

As the twist expansion starts to be applicable only above  $Q^2 \sim 1 \text{ GeV}^2$  the cut  $Q^2 \geq 1 \text{ GeV}^2$  on the data is applied throughout.

MINUIT program [45] is used to minimize two variables

$$\chi^2 = \left| \frac{F_2^{exp} - F_2^{teor}}{\Delta F_2^{exp}} \right|^2, \quad \chi_{slope}^2 = \left| \frac{D^{exp} - D^{teor}}{\Delta D^{exp}} \right|^2,$$

$D = d \ln F_2 / d \ln Q^2$ . The quality of the fits is characterized by  $\chi^2 / DOF$  for the structure function  $F_2$ . Analysis is also performed for the SF slope  $D$  that serves the purpose of checking the properties of fits (for more details see [2]).

We use free normalizations of the data for different experiments. For a reference set, the most stable deuterium BCDMS data at the value of the beam initial energy  $E_0 = 200 \text{ GeV}$  is used. With the other datasets taken to be a reference one the variation in the results is still negligible. In the case of the fixed normalization for each and all datasets the fits tend to yield a little bit worse  $\chi^2$ , just as in the previous studies.

## 5 Results

Since there is no gluons in the nonsinglet approximation the analysis is essentially easier to conduct, with the cut imposed on the Bjorken variable  $x \geq 0.25$  where gluon density is believed to be negligible.

Here we conduct separate and combined analyses of SLAC, BCDMS and NMC datasets obtained with hydrogen and deuterium targets. The cut on  $x$  is imposed in a combination with those placed on the  $y = (E_0 - E) / E_0$  variable ( $E_0$  and  $E$  are initial and final lepton energies, respectively) as follows:

$$y \geq 0.14 \quad \text{for} \quad 0.3 < x \leq 0.4$$

$$\begin{aligned}
y &\geq 0.16 && \text{for } 0.4 < x \leq 0.5 \\
y &\geq 0.23 && \text{for } 0.5 < x \leq 0.6 \\
y &\geq 0.24 && \text{for } 0.6 < x \leq 0.7 \\
y &\geq 0.25 && \text{for } 0.7 < x \leq 0.8,
\end{aligned}$$

which are meant to cut out those points with large systematic errors. Thus, upon imposing the cuts a complete dataset consists of 327 points in the case of hydrogen target and 288 — deuterium one. The starting point of the QCD evolution is taken to be  $Q_0^2 = 90 \text{ GeV}^2$ . This  $Q_0^2$  value is close to the average values of  $Q^2$  spanning the corresponding data. From earlier studies [2, 3] it follows that it is enough to limit the number of moments to be accounted for as in [19, 20]:  $N_{max} = 8$ . Also note that the cut  $0.25 \leq x \leq 0.8$  is imposed throughout.

To reduce the number of parameters, we perform two groups of fits. The first one is dealt within a variable-flavor-number-scheme (VFNS) [2] and the  $H_2$  and  $D_2$  experimental datasets analyzed simultaneously. The results for the second group are obtained within a fixed-flavor-number-scheme (FFNS) with an active number of flavors  $n_f = 4$  and the  $H_2$  and  $D_2$  experimental datasets considered separately.

## 5.1 VFNS case

All the results obtained within our reference VFNS [2] and in the cases of “naive”, APT, and “frozen” modifications of  $\alpha_s$  are gathered in a set of tables separately for each order of perturbation theory approximation and displayed in Figs. 1–3 separately for all these three cases.

**Table 1.** *LO values of the twist-four term  $\tilde{h}_4(x)$  (with statistic errors given) obtained in the analysis of the combined  $H_2 + D_2$  dataset within a VFNS and with various modifications of  $\alpha_s$*

$x$	Naive analyt. $\alpha_s$	APT-inspired $\alpha_s$	Frozen $\alpha_s$	Standard $\alpha_s$
0.275	$-0.121 \pm 0.008$	$-0.123 \pm 0.008$	$-0.204 \pm 0.011$	$-0.271 \pm 0.012$
0.35	$-0.055 \pm 0.007$	$-0.055 \pm 0.007$	$-0.167 \pm 0.017$	$-0.257 \pm 0.017$
0.45	$0.119 \pm 0.012$	$0.119 \pm 0.012$	$-0.021 \pm 0.031$	$-0.144 \pm 0.030$
0.55	$0.422 \pm 0.022$	$0.422 \pm 0.023$	$0.211 \pm 0.053$	$0.051 \pm 0.049$
0.65	$0.870 \pm 0.060$	$0.866 \pm 0.059$	$0.558 \pm 0.095$	$0.364 \pm 0.088$
0.75	$1.322 \pm 0.117$	$1.336 \pm 0.112$	$0.917 \pm 0.152$	$0.709 \pm 0.138$
$\chi^2/DOF$	0.93	0.93	0.91	0.94
$\chi_{slope}^2/DOF$	2.30	2.35	2.15	2.60
$\alpha_s(M_Z^2)$	0.1474	0.1474	0.1409	0.1400

**Table 2.** *NLO values of the twist-four term  $\tilde{h}_4(x)$  (with statistic errors given) obtained in the analysis of the combined  $H_2 + D_2$  dataset within a VFNS and with various modifications of  $\alpha_s$*

$x$	Naive analyt. $\alpha_s$	APT-inspired $\alpha_s$	Frozen $\alpha_s$	Standard $\alpha_s$
0.275	$-0.127 \pm 0.009$	$-0.129 \pm 0.007$	$-0.183 \pm 0.008$	$-0.229 \pm 0.010$
0.35	$-0.098 \pm 0.007$	$-0.024 \pm 0.009$	$-0.149 \pm 0.010$	$-0.218 \pm 0.016$
0.45	$0.014 \pm 0.012$	$0.187 \pm 0.013$	$0.010 \pm 0.019$	$-0.084 \pm 0.030$
0.55	$0.172 \pm 0.024$	$0.506 \pm 0.019$	$0.215 \pm 0.033$	$0.098 \pm 0.052$
0.65	$0.339 \pm 0.057$	$0.910 \pm 0.045$	$0.476 \pm 0.065$	$0.356 \pm 0.093$
0.75	$0.478 \pm 0.107$	$1.230 \pm 0.090$	$0.757 \pm 0.108$	$0.648 \pm 0.145$
$\chi^2/DOF$	0.85	0.84	0.97	1.02
$\chi_{slope}^2/DOF$	0.82	0.78	0.87	1.20
$\alpha_s(M_Z^2)$	0.1275	0.1224	0.1169	0.1152

**Table 3.** *NNLO values of the twist-four term  $\tilde{h}_4(x)$  (with statistic errors given) obtained in the analysis of the combined  $H_2 + D_2$  dataset within a VFNS and with various modifications of  $\alpha_s$*

$x$	Naive analyt. $\alpha_s$	APT-inspired $\alpha_s$	Frozen $\alpha_s$	Standard $\alpha_s$
0.275	$-0.171 \pm 0.006$	$-0.196 \pm 0.008$	$-0.149 \pm 0.006$	$-0.173 \pm 0.017$
0.35	$-0.160 \pm 0.008$	$-0.152 \pm 0.012$	$-0.129 \pm 0.013$	$-0.094 \pm 0.020$
0.45	$-0.044 \pm 0.018$	$0.030 \pm 0.022$	$-0.007 \pm 0.031$	$-0.110 \pm 0.015$
0.55	$0.085 \pm 0.033$	$0.269 \pm 0.038$	$0.116 \pm 0.062$	$-0.086 \pm 0.033$
0.65	$0.221 \pm 0.065$	$0.551 \pm 0.074$	$0.218 \pm 0.115$	$0.085 \pm 0.083$
0.75	$0.304 \pm 0.100$	$0.782 \pm 0.116$	$0.258 \pm 0.169$	$0.158 \pm 0.105$
$\chi^2/DOF$	0.98	1.02	0.97	0.92
$\chi_{slope}^2/DOF$	1.22	1.17	1.02	1.83
$\alpha_s(M_Z^2)$	0.1151	0.1125	0.1163	0.1159

From Tables 1–3 it is seen that in all the cases considered  $\chi^2/DOF$  shows good agreement between experimental data and theoretical predictions for the SF Mellin moments. In LO and NLO cases, the analytic and “frozen” modifications lead to some additional improvement of fits, namely,  $\chi^2/DOF$  in these cases is less than that in the standard case.

Since the quantity  $\chi_{slope}^2/DOF$  is inherently linked with the pQCD aspects to be observed in the data, it in this respect is very informative for it strongly varies from one approximation to the other thus indicating if there are any effects incompatible with the  $Q^2$  dependence in each  $x$ -bin assumed. It is seen that it, much like the  $\chi^2/DOF$  quantity, demonstrates similar tendency: in all the cases considered, the analytic and “frozen” modifications lead to improvement of fits. Certain improvement of the quality of fits is observed at the NLO level. In this approximation even the standard  $\alpha_s$  case leads to reasonable agreement for the slopes; furthermore, for all the infrared modifications it is seen that  $\chi_{slope}^2/DOF < 1$ . In the NNLO approximation the numbers for the slope in the case with a standard  $\alpha_s$  are not as good but the infrared modifications (especially the “frozen” one) lead to better agreement between theoretical and experimental results for the former quantity. It is difficult to pin down a reason for such a deterioration of this agreement (in the scheme with a standard  $\alpha_s$ ) when NNLO corrections are added. Because this effect is absent in the FFNS case (see the following subsection), we suppose that the exact equation given in (7) for the coupling constant is somehow in inconsistency with the NNLO expression for the heavy quark thresholds, which is in fact based on certain expansions of the coupling constant at the threshold crossing points (see, for example, [2]). We plan to study this fine effect elsewhere.

The QCD coupling decreases from LO through NNLO, which is in perfect agreement with other studies (see [36] and references therein); it is seen that the frozen modification gives the results closest to those for the standard  $\alpha_s$ . In the analytic cases the values of  $\alpha_s(M_Z^2)$  are higher in the first two orders of perturbation theory, with the maxima in the difference  $\Delta\alpha_s(M_Z^2)$  being 0.0123 and 0.0072 for the naive analytic and APT cases, respectively, observed at NLO. Thus, the differences are substantially greater than the values of the total experimental error  $\Delta^{total}\alpha_s(M_Z^2) = 0.0022$ , which was obtained in [2] by combining statistical and systematic errors in quadrature.

At the NNLO the APT procedure leads to lower  $\alpha_s(M_Z^2)$ , though in the naive case the  $\alpha_s(M_Z^2)$  value is closer to those obtained for the frozen and standard versions. Nevertheless, all the NNLO  $\alpha_s(M_Z^2)$  values, except for the APT case, are in good agreement within statistical errors, which were found to be  $\Delta^{stat}\alpha_s(M_Z^2) = 0.0007$  in our previous studies [2]. The APT-inspired QCD coupling constant is compatible with the rest within the total experimental error.

From Tables 1–3 and, particularly, Figs. 1–3 it is seen that in the cases of analytic and “frozen” coupling constants the twist-four corrections are larger compared to those in the case of a standard perturbative coupling constant, thus confirming the results obtained in [24]. For example, at  $x \sim 0.75$  the higher-twist corrections (HTCs) in the standard case are about twice as less than those obtained in the cases of analytic modifications in all orders considered. In the “frozen” case, the HTC values are compatible with those in

the standard case within statistical errors.<sup>9</sup>

The difference in the values of HT parameter for the naive analytic and frozen variants becomes moderate at the NLO level unlike the APT case. For the infrared modifications the HT terms are large and in the frozen and APT cases are compatible with the LO ones.

In the NNLO approximation the situation changes drastically. HT terms for all the cases, except for the APT case, are comparable with each other. HTCs in the latter case are still higher but they also strongly suppressed to compare with them in LO and NLO cases. Thus, at the NNLO level the twist-four corrections appear to be small for all the cases considered above.

The values for parameters in the parameterizations of the parton distributions (see Eq. (4)) for the cases corresponding to different coupling constant modifications are given in Table 4. From this table it is seen that the parameters in all the cases considered are close to each other.

Moreover, the parameter  $b$ , which is responsible for the large  $x$  fall of the PDF shape, is found to be around 4, that is in agreement with the quark counting rules [48], if we take into account the rise of  $b$  at large  $Q_0^2$  values used here (see Eq. (B2)).

**Table 4.** *The values of PDF parameters obtained within a VFNS and with various modifications  $\alpha_s$  in the case of the combined  $H_2 + D_2$  dataset analyzed*

Par.	Naive analyt. $\alpha_s$			APT-inspired $\alpha_s$			Frozen $\alpha_s$			Standard $\alpha_s$		
	LO	NLO	NNLO	LO	NLO	NNLO	LO	NLO	NNLO	LO	NLO	NNLO
A( $H_2$ )	2.43	2.65	2.54	2.46	2.54	2.51	2.48	2.63	2.55	2.53	2.62	2.57
b( $H_2$ )	3.73	4.06	4.16	3.72	4.07	4.14	3.71	4.03	4.16	3.71	4.02	4.13
d( $H_2$ )	5.26	4.72	6.13	5.13	5.61	6.29	5.06	4.95	5.98	4.92	5.07	5.60
A( $D_2$ )	2.29	2.64	2.43	2.32	2.52	2.45	2.31	2.57	2.48	2.32	2.52	2.50
b( $D_2$ )	3.77	4.09	4.21	3.76	4.11	4.19	3.75	4.07	4.20	3.75	4.07	4.15
d( $D_2$ )	3.07	2.79	3.72	2.97	3.21	3.66	2.99	2.96	3.57	2.95	3.11	3.39

## 5.2 FFNS case

For comparison let's present the values of PDF parameters obtained within the FFNS ( $n_f = 4$ ) in the analyses of the hydrogen data for the versions of the strong coupling constant discussed above, with the addition for the case of FAPT-inspired modification of  $\alpha_s$ .

Here we have no threshold transitions for QCD coupling and PDF Mellin moments and, hence, are able to consider the hydrogen and deuterium datasets separately. From Table 5, we see that all the parameters in the parameterizations of the parton distributions (see Eq. (4)) for the cases corresponding to different coupling constant modifications are close to each other in all the cases considered. As was already discussed in the previous subsection, the parameter  $b \sim 4$ , that is in agreement with the quark counting rules [48], if we take into account its certain rise at large  $Q_0^2$  values.

**Table 5.** *The values of PDF parameters obtained within the FFNS ( $n_f = 4$ ) for various modifications of  $\alpha_s$  in the case of  $H_2$  and  $D_2$  datasets analyzed separately*

Par.	Naive analyt. $\alpha_s$			APT $\alpha_s$			Frozen $\alpha_s$			FAPT $\alpha_s$		
	LO	NLO	NNLO	LO	NLO	NNLO	LO	NLO	NNLO	LO	NLO	NNLO
A( $H_2$ )	2.30	2.58	2.49	2.30	2.52	2.42	2.32	2.57	2.49	1.68	2.55	2.47
b( $H_2$ )	3.74	4.06	4.18	3.74	4.08	4.19	3.74	4.04	4.18	3.74	4.05	4.18
d( $H_2$ )	5.63	5.30	6.46	5.63	5.82	6.91	5.70	5.36	6.38	5.90	5.50	6.54
A( $D_2$ )	2.42	2.75	2.60	2.42	2.57	2.51	2.38	2.66	2.62	2.34	2.65	2.58
b( $D_2$ )	3.73	4.05	4.19	3.73	4.08	4.20	3.72	4.02	4.17	3.72	4.03	4.17
d( $D_2$ )	2.61	2.47	3.15	2.61	2.98	3.42	2.72	2.61	3.10	2.82	2.64	3.18

<sup>9</sup>For the results to be discernible, Figs. 1–4 and 6–7 contain statistical errors for the infrared modifications only. The magnitude of the errors is on par in the standard case and is not shown.

By using the case of “naively analytized”  $\alpha_s$  it is demonstrated in Fig. 5 that the values of HTCs obtained for the  $n_f = 4$  and  $n_f = 5$  cases in the FFNS are very much alike.

In order to be able to assess the difference among the cases with frozen, FAPT and standard versions for the strong coupling constant let’s present the tables with the HT values obtained within FFNS ( $n_f = 4$ ).

**Table 6.** LO values of the twist-four term obtained within the FFNS ( $n_f = 4$ ) and with various modifications of  $\alpha_s$  in the separate analyses of  $H_2$  and  $D_2$  datasets

$x$	FAPT-inspired $\alpha_s$ ( $\pm$ stat)		Frozen $\alpha_s$ ( $\pm$ stat)		Standard $\alpha_s$ ( $\pm$ stat)	
	$h_4(x)$ for $H_2$	$h_4(x)$ for $D_2$	$h_4(x)$ for $H_2$	$h_4(x)$ for $D_2$	$h_4(x)$ for $H_2$	$h_4(x)$ for $D_2$
0.275	-0.221 $\pm$ 0.011	-0.206 $\pm$ 0.010	-0.183 $\pm$ 0.012	-0.167 $\pm$ 0.015	-0.235 $\pm$ 0.012	-0.229 $\pm$ 0.011
0.35	-0.187 $\pm$ 0.014	-0.134 $\pm$ 0.009	-0.160 $\pm$ 0.018	-0.104 $\pm$ 0.022	-0.232 $\pm$ 0.021	-0.192 $\pm$ 0.010
0.45	0.002 $\pm$ 0.023	0.072 $\pm$ 0.016	-0.023 $\pm$ 0.037	0.055 $\pm$ 0.042	-0.130 $\pm$ 0.038	-0.072 $\pm$ 0.018
0.55	0.332 $\pm$ 0.034	0.462 $\pm$ 0.026	0.189 $\pm$ 0.065	0.330 $\pm$ 0.074	0.049 $\pm$ 0.065	0.158 $\pm$ 0.029
0.65	1.001 $\pm$ 0.063	1.078 $\pm$ 0.068	0.610 $\pm$ 0.117	0.701 $\pm$ 0.132	0.455 $\pm$ 0.111	0.495 $\pm$ 0.067
0.75	2.031 $\pm$ 0.131	1.701 $\pm$ 0.142	1.177 $\pm$ 0.207	0.913 $\pm$ 0.206	1.003 $\pm$ 0.182	0.677 $\pm$ 0.128
$\chi^2/DOF$	0.98	0.77	0.94	0.75	0.98	0.78
$\chi_{slope}^2/DOF$	1.47	2.23	1.25	1.93	1.58	2.45
$\alpha_s(M_Z^2)$	0.1394	0.1426	0.1387	0.1388	0.1376	0.1383

**Table 7.** NLO values of the twist-four term obtained within the FFNS ( $n_f = 4$ ) and with various modifications of  $\alpha_s$  in the separate analyses of  $H_2$  and  $D_2$  datasets

$x$	FAPT-inspired $\alpha_s$ ( $\pm$ stat)		Frozen $\alpha_s$ ( $\pm$ stat)		Standard $\alpha_s$ ( $\pm$ stat)	
	$h_4(x)$ for $H_2$	$h_4(x)$ for $D_2$	$h_4(x)$ for $H_2$	$h_4(x)$ for $D_2$	$h_4(x)$ for $H_2$	$h_4(x)$ for $D_2$
0.275	-0.205 $\pm$ 0.012	-0.209 $\pm$ 0.019	-0.154 $\pm$ 0.011	-0.147 $\pm$ 0.014	-0.200 $\pm$ 0.012	-0.206 $\pm$ 0.015
0.35	-0.194 $\pm$ 0.017	-0.165 $\pm$ 0.026	-0.147 $\pm$ 0.016	-0.099 $\pm$ 0.021	-0.219 $\pm$ 0.019	-0.189 $\pm$ 0.024
0.45	-0.067 $\pm$ 0.030	-0.027 $\pm$ 0.039	-0.058 $\pm$ 0.037	0.013 $\pm$ 0.044	-0.169 $\pm$ 0.041	-0.122 $\pm$ 0.048
0.55	0.160 $\pm$ 0.044	0.252 $\pm$ 0.052	0.069 $\pm$ 0.067	0.204 $\pm$ 0.078	-0.078 $\pm$ 0.072	0.018 $\pm$ 0.083
0.65	0.635 $\pm$ 0.071	0.702 $\pm$ 0.083	0.317 $\pm$ 0.118	0.432 $\pm$ 0.139	0.153 $\pm$ 0.123	0.207 $\pm$ 0.143
0.75	1.512 $\pm$ 0.130	1.243 $\pm$ 0.137	0.723 $\pm$ 0.204	0.509 $\pm$ 0.210	0.534 $\pm$ 0.205	0.251 $\pm$ 0.212
$\chi^2/DOF$	0.91	0.70	0.89	0.71	0.92	0.73
$\chi_{slope}^2/DOF$	1.08	1.35	0.92	1.27	1.23	1.68
$\alpha_s(M_Z^2)$	0.1220	0.1261	0.1200	0.1201	0.1192	0.1199

**Table 8.** NNLO values of the twist-four term obtained within the FFNS ( $n_f = 4$ ) and with various modifications of  $\alpha_s$  in the separate analyses of  $H_2$  and  $D_2$  datasets

$x$	FAPT-inspired $\alpha_s$ ( $\pm$ stat)		Frozen $\alpha_s$ ( $\pm$ stat)		Standard $\alpha_s$ ( $\pm$ stat)	
	$h_4(x)$ for $H_2$	$h_4(x)$ for $D_2$	$h_4(x)$ for $H_2$	$h_4(x)$ for $D_2$	$h_4(x)$ for $H_2$	$h_4(x)$ for $D_2$
0.275	-0.168 $\pm$ 0.010	-0.175 $\pm$ 0.013	-0.119 $\pm$ 0.011	-0.116 $\pm$ 0.012	-0.158 $\pm$ 0.020	-0.161 $\pm$ 0.012
0.35	-0.181 $\pm$ 0.015	-0.155 $\pm$ 0.020	-0.112 $\pm$ 0.010	-0.072 $\pm$ 0.017	-0.166 $\pm$ 0.021	-0.146 $\pm$ 0.017
0.45	-0.130 $\pm$ 0.037	-0.095 $\pm$ 0.045	-0.049 $\pm$ 0.018	0.012 $\pm$ 0.042	-0.156 $\pm$ 0.036	-0.108 $\pm$ 0.043
0.55	-0.056 $\pm$ 0.065	0.023 $\pm$ 0.079	0.007 $\pm$ 0.031	0.129 $\pm$ 0.080	-0.157 $\pm$ 0.079	-0.035 $\pm$ 0.080
0.65	0.126 $\pm$ 0.111	0.162 $\pm$ 0.133	0.106 $\pm$ 0.058	0.209 $\pm$ 0.145	-0.061 $\pm$ 0.127	0.022 $\pm$ 0.142
0.75	0.419 $\pm$ 0.178	0.163 $\pm$ 0.191	0.240 $\pm$ 0.116	0.088 $\pm$ 0.213	0.049 $\pm$ 0.209	-0.117 $\pm$ 0.207
$\chi^2/DOF$	0.89	0.70	0.87	0.68	0.89	0.71
$\chi_{slope}^2/DOF$	0.97	1.22	0.68	0.85	0.97	1.28
$\alpha_s(M_Z^2)$	0.1183	0.1197	0.1180	0.1184	0.1176	0.1176

Just like in the previous subsection it is seen from Tables 6–8 that in all the cases at hand, we have good agreement between the experimental data and theoretical predictions. Once again, in all the cases considered, excluding LO FAPT, the analytic and frozen modifications lead to slight improvement of fits, that is  $\chi^2/DOF$  and  $\chi_{slope}^2/DOF$  are found to be smaller in these cases than those for the standard  $\alpha_s$ , and the QCD coupling constant decreases when we move from LO through NNLO.

Also note that contrary to what was observed in the previous subsection here the quantity  $\chi_{slope}^2/DOF$  steadily decreases when we proceed step by step from LO to NLO

and then to NNLO level. Respectively, here the smaller values of  $\chi_{slope}^2/DOF$  are observed for the “frozen” case as well.

The values of coupling constants are very similar, especially for the “frozen” and standard versions. In the analytic cases, the central values of  $\alpha_s(M_Z^2)$  are little higher, mostly in the first two orders of perturbation theory.

In the NNLO, all the  $\alpha_s(M_Z^2)$  values, except for the analytic one, are in good agreement within statistical errors. As earlier, the analytic QCD coupling is in agreement with the rest within the total experimental error.

Similarly to the previous subsection we note in Figs. 4, 6, 8 <sup>10</sup> appreciable difference between HTCs obtained in the standard and analytic cases in the first two orders of perturbation theory. The difference in the cases of a “frozen” and standard  $\alpha_s$  is not as large; the values of HT terms are in agreement within statistical errors.

In the NNLO, the situation is over again changed considerably. In all the cases of infrared modifications considered, the HTCs are small. Similarly to the previous subsection they are not compatible with zero at  $x \sim 0.75$ , while the HT terms in standard QCD are compatible with zero and, at the same time, in agreement with all the cases considered within statistical errors.

Then, at NNLO we can see agreement between standard QCD and its infrared modifications for QCD coupling  $\alpha_s(M_Z^2)$ , as well as for the respective HTCs (as a rule) within statistical errors.

## 6 Conclusions

The pattern of separating perturbative QCD and HT corrections may be different in different orders of perturbation theory, as well as in some resummations based on several first orders, and for certain modifications of the strong coupling constant as well. In the present paper, we studied consequences of the infrared modifications of the QCD coupling constant — the so-called “frozen” and “analytized” versions. In the last case we considered three different options:

- a simple modification of the strong coupling constant [14] without rearrangement of a perturbation series;
- an application of the ordinary analytic perturbation theory (see [24]) to the “moments”  $\mu_n^{NS}(Q^2)$  given in (22);
- impact of the fractional analytic perturbation theory [39] applied directly to the Mellin moments  $M_n^{NS}(Q^2)$ .

To test all these modifications, the Jacobi polynomial expansion method developed in [18, 19, 20] was used to perform analysis of  $Q^2$ -evolution of the DIS structure function  $F_2$  by fitting all existing to date reliable fixed-target experimental data that satisfy the cut  $x \geq 0.25$ . To the best of our knowledge, this is the first application of the FAPT results to the fits of the DIS structure functions.

From the results obtained we conclude that in the first two orders of perturbation theory the value of the QCD coupling constant at the reference point  $\alpha_s(M_Z^2)$  is larger with respect to that in the standard case, for all versions of the analytic perturbation theory. An increase in the central values of  $\alpha_s(M_Z^2)$  is smaller in the NNLO approximation, much like the case of the “frozen” version of  $\alpha_s$ . Nevertheless, in all the cases the  $\alpha_s(M_Z^2)$  values agree mostly within total experimental errors. For the NNLO case, the results are as a rule compatible between each other within statistical errors. Also, we note that within statistical errors only (in our case  $\Delta^{stat}\alpha_s(M_Z^2) = 0.0007$  [2]) all the NNLO results for

---

<sup>10</sup>Since the magnitude of HTCs is a bit higher for the hydrogen dataset (see, for example, our recent paper [2]) we consider only this case.

$\alpha_s(M_Z^2)$  in the FFNS case (see Table 8) are too compatible with the world average value for the coupling constant presented in the review [49]<sup>11</sup>:

$$\alpha_s(M_Z^2) = 0.1184 \pm 0.0007.$$

It is also observed that the values of the twist-four corrections in the first two orders of perturbation theory are higher than those in the standard case, particularly for all versions of the analytic perturbation theory. This observation is in complete agreement with recent studies [24] of the Bjorken sum rules, where it was shown that there is a reduction of higher HT terms, starting with the twist-six ones. Unfortunately, here we are not able to study the twist-four and twist-six corrections simultaneously since their contributions are strongly correlated.

In the NNLO, all the cases of infrared modifications of the QCD coupling feature nonzero although rather small twist-four corrections. Whereas in the case of the standard QCD approach, the HT terms are close to zero at large  $x$  values. However, the NNLO HTCs for all the cases considered are compatible between each other within statistical errors. In principle, the main difference between standard QCD and its analytic and “frozen” modifications is in the strong suppression of the higher twist corrections in NLO and NNLO orders of perturbation theory, respectively.

What is interesting to look for further in the study is the consideration of the combined nonsinglet and singlet analyses using the DIS experimental data within an entire  $x$  region, as well as an application of certain resummation-like Grunberg effective charge methods [38] (as was done in [37] in the NLO approximation) and the “frozen” [13]<sup>12</sup> and analytic [31] versions of the strong coupling constant (see [35, 30, 24] for recent studies in this direction). The effect of N<sup>3</sup>LO corrections would also seem to be important to account for in the subsequent investigations, as well as an extension of the FAPT model results for  $\alpha_s$  to the VFNS case.

## 7 Acknowledgments

The work was supported by the RFBR grant No.10-02-01259-a. We are grateful to S.V. Mikhailov, D.B. Stamenov and O.V. Teryaev for useful discussions.

## 8 Appendix A

Here we present a simple evaluation of the equation given in (31).

Using Sec. II.5 in [46], we have

$$\text{Li}_{1-\nu}(z) = \frac{z}{\Gamma(1-\nu)} \int_0^\infty \frac{t^{-\nu} dt}{e^t - z} \quad (\nu < 1). \quad (\text{A1})$$

Upon substituting  $t = \ln(1/\xi)$ , we obtain for the r.h.s. of Eq. (A1)

$$\frac{z}{\Gamma(1-\nu)} \int_0^1 \frac{d\xi}{1-z\xi} \ln^{-\nu} \left( \frac{1}{\xi} \right) \quad (\nu < 1), \quad (\text{A2})$$

---

<sup>11</sup>It should be mentioned that this analysis was carried out over the data coming from the various experiments and in different orders of perturbation theory, i.e. from NLO up to N<sup>3</sup>LO.

<sup>12</sup>There are a lot of “frozen” versions of the strong coupling constant (see, for example, the list of references in [30]).

In order to extend Eq. (A2) to the values of  $\nu > 1$ , it is useful to consider a series representation (29) for  $\nu = N + \delta$ :

$$\text{Li}_{1-N-\delta}(z) = \sum_{m=1}^{\infty} m^{N+\delta-1} z^m = \left(z \frac{d}{dz}\right)^N \sum_{m=1}^{\infty} m^{\delta-1} z^m = \left(z \frac{d}{dz}\right)^N \text{Li}_{1-\delta}(z). \quad (\text{A3})$$

Taking the representation (A2) for the r.h.s. of (A3), we have

$$\text{Li}_{1-N-\delta}(z) = \left(z \frac{d}{dz}\right)^N \left[ \frac{z}{\Gamma(1-\delta)} \int_0^1 \frac{d\xi}{1-z\xi} \ln^{-\delta} \left(\frac{1}{\xi}\right) \right] \quad (0 < \delta < 1). \quad (\text{A4})$$

## 9 Appendix B

Consider the large  $x$  asymptotic [47] of SF  $F_2(x, Q^2)$  (for simplicity we restrict ourselves to the LO approximation)

$$F_2(x, Q^2) \sim (1-x)^{b(a_s^{(0)}(Q^2))}, \quad (\text{B1})$$

where

$$b(a_s^{(0)}(Q^2)) = b_0 - \tilde{d} \ln(a_s^{(0)}(Q^2)), \quad \tilde{d} = \frac{16}{3\beta_0},$$

and  $b_0$  is some constant which can be obtained from the quark counting rules [48].

The  $Q^2$ -dependent part in the r.h.s. of (B1) can be represented as follows:

$$(1-x)^{-\tilde{d} \ln(a_s^{(0)}(Q^2))} = [a_s^{(0)}(Q^2)]^{-\tilde{d} \ln(1-x)}.$$

Performing the ‘‘analytization’’ procedure and using (14), we have

$$\left(a_s^{(0)}(Q^2) - \frac{1}{\beta_0} \frac{\Lambda_{(0)}^2}{Q^2 - \Lambda_{(0)}^2}\right)^{-\tilde{d} \ln(1-x)} \approx [a_s^{(0)}(Q^2)]^{-\tilde{d} \ln(1-x)} \left[1 + \frac{\tilde{d} \ln(1-x)}{\beta_0 a_s^{(0)}(Q^2)} \frac{\Lambda_{(0)}^2}{Q^2 - \Lambda_{(0)}^2}\right]. \quad (\text{B2})$$

From this expression it follows that the power corrections, which were generated by the ‘‘analytization’’ of the coupling constant, have the opposite sign as compared to the twist-four corrections at large  $x$  and, moreover, demonstrate a different asymptotic behavior. These corrections (taken with the additional sign ‘‘-’’) increase like  $\ln(1-x)$  while the twist-four corrections behave like  $1/(1-x)$  (see [27] and discussions therein). This difference in sign between these corrections leads to the larger twist-four corrections in the present analysis than those given in [2].

## References

- [1] M. Beneke, Phys. Rept. **317** (1999) 1.
- [2] B.G. Shaikhatdenov, A.V. Kotikov, V.G. Krivokhizhin, and G. Parente, Phys. Rev. **D81** (2010) 034008.
- [3] V.G. Krivokhizhin, A.V. Kotikov, Yad.Fiz. **68** (2005) 1935 [Phys.Atom.Nucl. **68** (2005) 1873].
- [4] SLAC Collab., L.W. Whitlow et al., Phys. Lett. **B282** (1992) 475.
- [5] SLAC Collab., L.W. Whitlow, Ph.D. Thesis Stanford University, SLAC report 357 (1990).
- [6] NMC Collab., M. Arneodo et al., Nucl. Phys. **B483** (1997) 3.

- [7] BCDMS Collab., A.C. Benevenuti et al., Phys. Lett. **B223** (1989) 485.
- [8] BCDMS Collab., A.C. Benevenuti et al., Phys. Lett. **B237** (1990) 592.
- [9] BCDMS Collab., A.C. Benevenuti et al., Phys. Lett. **B195** (1987) 91.
- [10] J.A.M. Vermaseren, A. Vogt, S. Moch, Nucl.Phys.**B688** (2004) 101; hep-ph/0403192
- [11] J.A.M. Vermaseren, A. Vogt, S. Moch, Nucl.Phys.**B724** (2005) 3; hep-ph/0504242
- [12] V.G. Krivokhizhin, A.V. Kotikov, Phys.Part.Nucl. **40** (2009) 1059.
- [13] B. Badelek, J. Kwiecinski, and A. Stasto, Z. Phys. **C74** (1997) 297.
- [14] D.V. Shirkov and I.L. Solovtsov, Phys. Rev. Lett. **79** (1997) 1209.
- [15] M. Virchaux and A. Milsztajn, Phys. Lett. **B274** (1992) 221.
- [16] A.D. Martin, W.J. Stirling, R.S. Thorne, and G. Watt, Phys. Lett. **B652** (2007) 292; A.D. Martin, R.G. Roberts, W.J. Stirling and R.S. Thorne, Eur. Phys. J. **C28** (2003) 455; Eur. Phys. J. **C35** (2004) 325; P. Jimenez-Delgado and E. Reya, Phys. Rev. **D79** (2009) 074023; M Gluck, C. Pisano and E. Reya, Phys. Rev. **D77** (2008) 074002; M Gluck, P. Jimenez-Delgado and E. Reya, Eur. Phys. J. **C53** (2008) 355; STEQ Collab., W.K. Tung, H.Lai, A. Belyaev, J. Pumplin, D. Sturm, and C.-P. Yuan, JHEP **0702** (2007) 053; H.Lai, P.M. Nadolsky, J. Pumplin, D. Sturm, W.K. Tung, and C.-P. Yuan, JHEP **0704** (2007) 089; S. Kretzer, H.Lai, F.I. Olness, and W.K. Tung, Phys. Rev. **D69** (2004) 114005; S. Alekhin, JETP Lett. **82** (2005) 628; Phys. Rev. **D68** (2003) 014002; JHEP **0302** (2003) 015; Phys. Lett. **B519** (2001) 57.
- [17] V.N. Gribov and L.N. Lipatov, Sov. J. Nucl. Phys. **15** (1972) 438; L.N. Lipatov, Sov. J. Nucl. Phys. **20** (1975) 94; G. Altarelli and G. Parisi, Nucl. Phys. **B126** (1977) 298; Yu.L. Dokshitzer, JETP **46** (1977) 641.
- [18] G. Parisi and N. Surlas, Nucl. Phys. **B151** (1979) 421; I.S. Barker, C.B. Langensiepen and G. Shaw, Nucl. Phys. **B186** (1981) 61; I.S. Barker, B.R. Martin, and G. Shaw, Z. Phys. **C19** (1983) 147; I.S. Barker and B.R. Martin, Z. Phys. **C24** (1984) 255.
- [19] V.G. Krivokhizhin, S.P. Kurlovich, V.V. Sanadze, I.A. Savin, A.V. Sidorov and N.B. Skachkov, Z. Phys. **C36** (1987) 51.
- [20] V.G. Krivokhizhin, S.P. Kurlovich, R. Lednicky, S. Nemecek, V.V. Sanadze, I.A. Savin, A.V. Sidorov and N.B. Skachkov, Z. Phys. **C48** (1990) 347.
- [21] A. Buras, Rev. Mod. Phys. **52** (1980) 199.
- [22] G. Parente, A.V. Kotikov and V.G. Krivokhizhin, Phys. Lett. **B333** (1994) 190.
- [23] A.L. Kataev, G. Parente and A.V. Sidorov, Nucl. Phys. **B573** (2000) 405.
- [24] R.S. Pasechnik, D.V. Shirkov, and O.V. Teryaev, Phys. Rev. **D78** (2008) 071902; R.S. Pasechnik, D.V. Shirkov, O.V. Teryaev, O.P. Solovtsova, and V.L. Khandramai, Phys. Rev. **D81** (2010) 016010.
- [25] D.I. Kazakov and A.V. Kotikov, Nucl.Phys. **B307** (1988) 791; (E: **345**, 299 (1990)).
- [26] A.V. Kotikov and V.N. Velizhanin, hep-ph/0501274; A.V. Kotikov, Phys. Atom. Nucl. **57** (1994) 133.
- [27] F.J. Yndurain, *Quantum Chromodynamics (An Introduction to the Theory of Quarks and Gluons)*, Berlin, Springer-Verlag (1983).
- [28] A.L. Kataev, A.V. Kotikov, G. Parente and A.V. Sidorov, Phys. Lett. **B388** (1996) 179; Phys. Lett. **B417** (1998) 374; A.V. Sidorov, Phys. Lett. **B389** (1996) 379.

- [29] Y. L. Dokshitzer and D. V. Shirkov, *Z. Phys. C* **67** (1995) 449;  
A. V. Kotikov, *Phys. Lett. B* **338** (1994) 349.  
S. J. Brodsky, V. S. Fadin, V. T. Kim, L. N. Lipatov and G. B. Pivovarov, *JETP Lett.* **70** (1999) 155 [arXiv:hep-ph/9901229].
- [30] A.V. Kotikov, A.V. Lipatov, and N.P. Zotov, *J. Exp. Theor. Phys.* **101** (2005) 811.
- [31] I. L. Solovtsov and D. V. Shirkov, *Theor. Math. Phys.* **120** (1999) 1220 [*Teor. Mat. Fiz.* **120** (1999) 482] [arXiv:hep-ph/9909305].
- [32] G. Cvetic and C. Valenzuela, *Braz. J. Phys.* **38** (2008) 371 [arXiv:0804.0872 [hep-ph]];  
A.P. Bakulev, *Phys. Part. Nucl.* **40** (2009) 715.
- [33] A. V. Nesterenko and C. Simolo, arXiv:1001.0901[hep-ph].
- [34] A. Yu. Illarionov, A. V. Kotikov and G. Parente Bermudez, *Phys. Part. Nucl.* **39** (2008) 307 [arXiv:hep-ph/0402173].
- [35] G. Cvetic, A. Y. Illarionov, B. A. Kniehl and A. V. Kotikov, *Phys. Lett.* **B679** (2009) 350.
- [36] A. V. Kotikov, *Phys. Part. Nucl.* **38** (2007) 1 [Erratum-ibid. **38** (2007) 828].
- [37] V.I. Vovk, *Z. Phys.* **C47** (1990) 57;  
A.V. Kotikov, G. Parente and J. Sanchez Guillen, *Z. Phys.* **C58** (1993) 465.
- [38] G. Grunberg, *Phys. Lett.* **B95** (1980) 70; *Phys. Rev.* **D29** (1984) 2315.
- [39] A. P. Bakulev, S. V. Mikhailov and N. G. Stefanis, *Phys. Rev. D* **72** (2005) 074014 [Erratum-ibid. *D* **72** (2005) 119908] [arXiv:hep-ph/0506311]; A. P. Bakulev, S. V. Mikhailov and N. G. Stefanis, *Phys. Rev. D* **75** (2007) 056005. [Erratum-ibid. *D* **77** (2008) 079901] [arXiv:hep-ph/0607040].
- [40] F.J. Yndurain, *Phys. Lett.* **B74** (1978) 68.
- [41] A. Gonzalez-Arroyo, C. Lopez, *Nucl.Phys.* **B166** (1980) 429;  
A. Gonzalez-Arroyo, C. Lopez, F.J. Yndurain, *Nucl.Phys.* **B174** (1980) 474.
- [42] B. Escobles, M.J. Herrero, C. Lopez, and F.J. Yndurain, *Nucl. Phys.* **B242** (1984) 329;  
D.I. Kazakov and A.V. Kotikov, *Sov. J. Nucl. Phys.* **46** (1987) 1057.
- [43] J. Santiago and F.J. Yndurain, *Nucl. Phys.* **B563** (1999) 45.
- [44] A.L. Kataev, G. Parente and A.V. Sidorov, *Phys. Part. Nucl.* **34** (2003) 20.
- [45] F. James and M. Ross, "MINUIT", CERN Computer Center Library, D 505, Geneve, 1987.
- [46] A.P. Prudnikov, Yu.A. Brychkov, and O.I. Marichev, *Integrals and Series, Vol. 3: More Special Functions, New York: Gordon and Breach* (1989) 800 p.
- [47] D.I. Gross, *Phys. Rev. Lett.* **32** (1974) 1071;  
D.I. Gross and S.B. Treiman, *Phys. Rev. Lett.* **32** (1974) 1145.
- [48] V.A. Matveev, R.M. Muradian and A.N. Tavkhelidze, *Lett. Nuovo Cim.* **7** (1973) 719;  
S.J. Brodsky and G.R. Farrar, *Phys. Rev. Lett.* **31** (1973) 1153;  
S.J. Brodsky, J. Ellis, E. Cardi, M. Karliner and M.A. Samuel, *Phys. Rev.* **D56** (1997) 6980.
- [49] S. Bethke, *Eur. Phys. J. Phys.* **C64** (2009) 689.

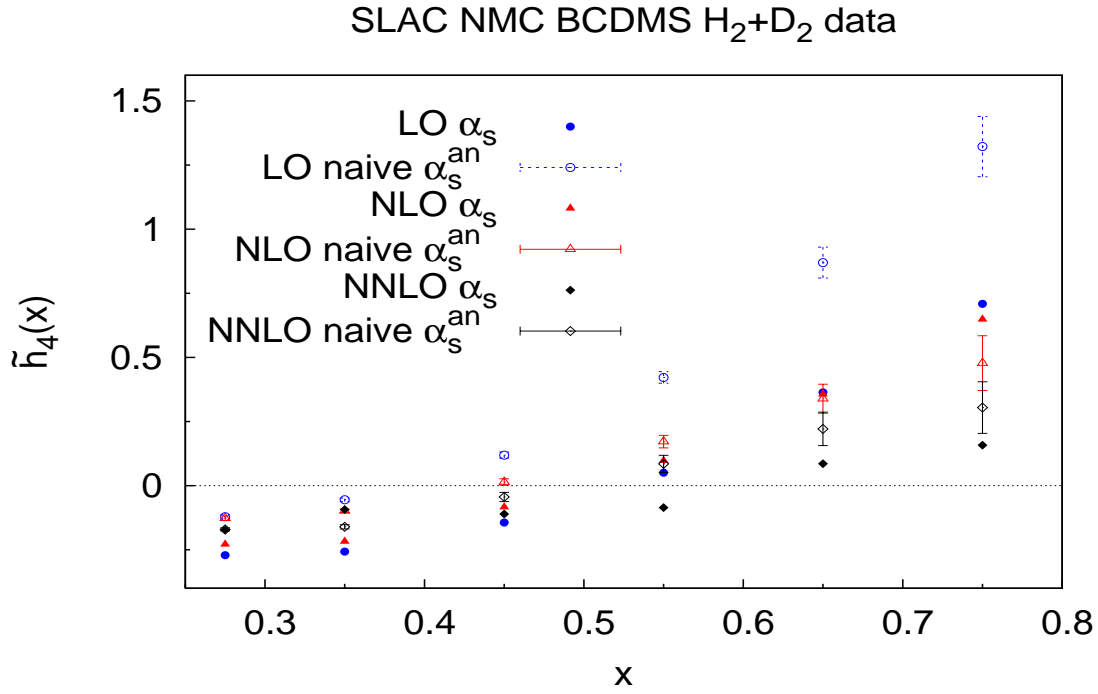


Figure 1: Comparison of the HTC parameter  $\tilde{h}_4(x)$  obtained in LO, NLO and NNLO for hydrogen data (the bars show statistical errors) between our reference VFNS with a standard perturbative  $\alpha_s$  [2] and that with naive analytic  $\alpha_s$ .

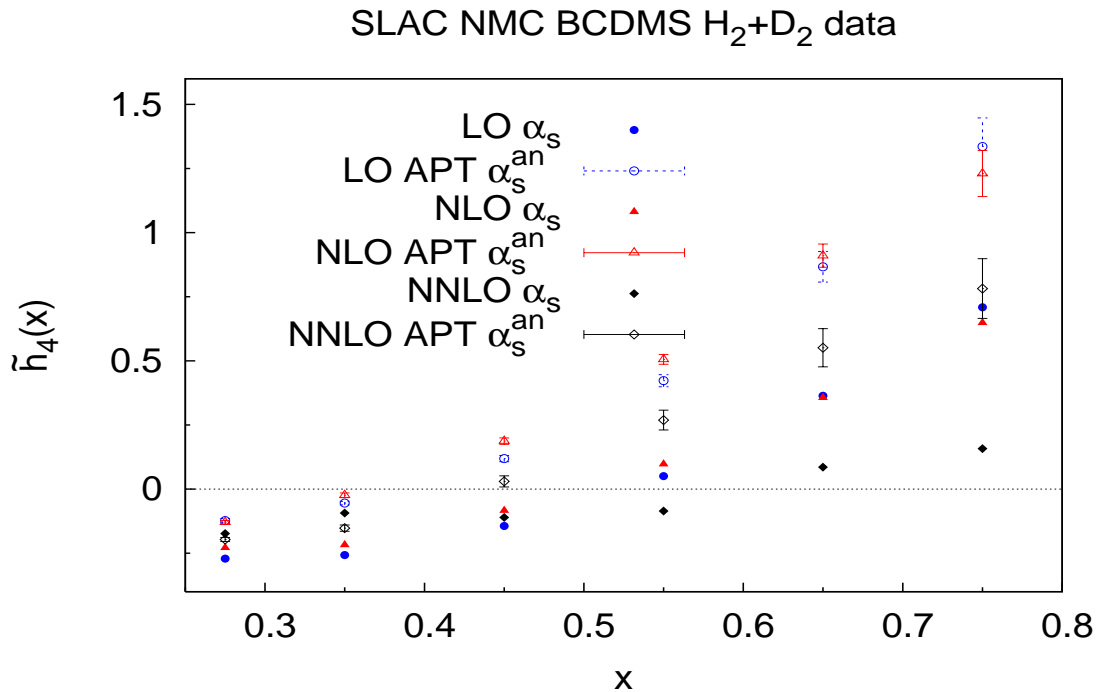


Figure 2: Comparison of the HTC parameter  $\tilde{h}_4(x)$  obtained in LO, NLO and NNLO for hydrogen data between a VFNS and that with APT-inspired  $\alpha_s$ .

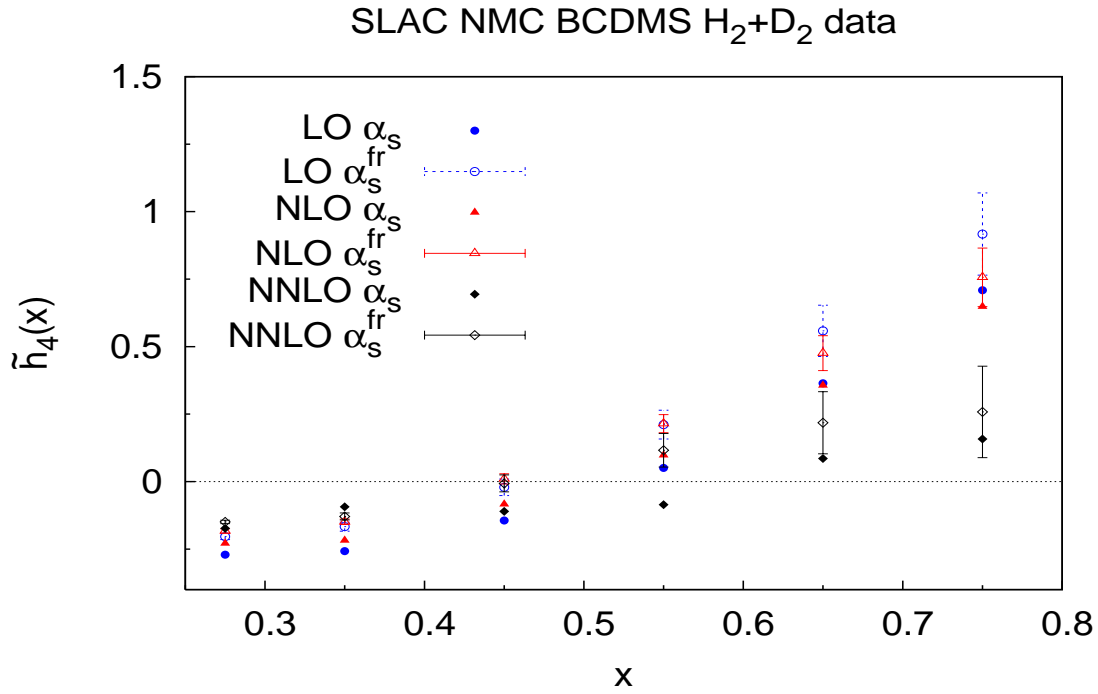


Figure 3: Comparison of the HTC parameter  $\tilde{h}_4(x)$  obtained at LO, NLO and NNLO for hydrogen data within a VFNS between the cases with a standard perturbative and “frozen”  $\alpha_s$ .

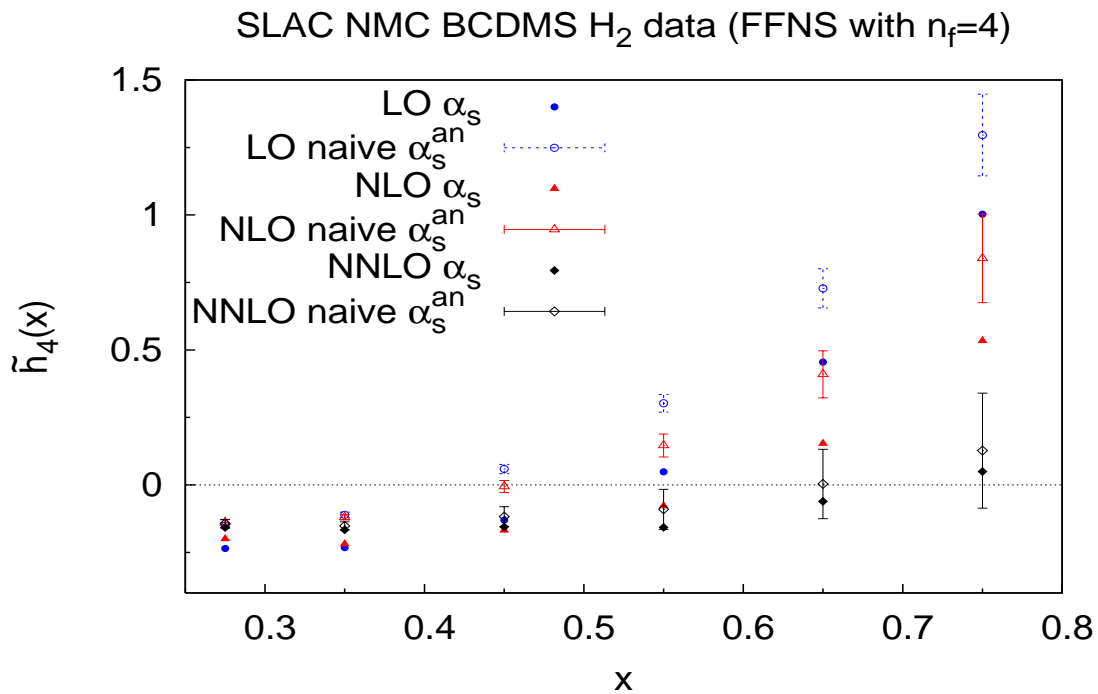


Figure 4: Comparison of the HTC parameter  $\tilde{h}_4(x)$  obtained in LO, NLO and NNLO for hydrogen data within a FFNS ( $n_f = 4$ ) between the cases with a standard perturbative and naively analyzed  $\alpha_s$ .

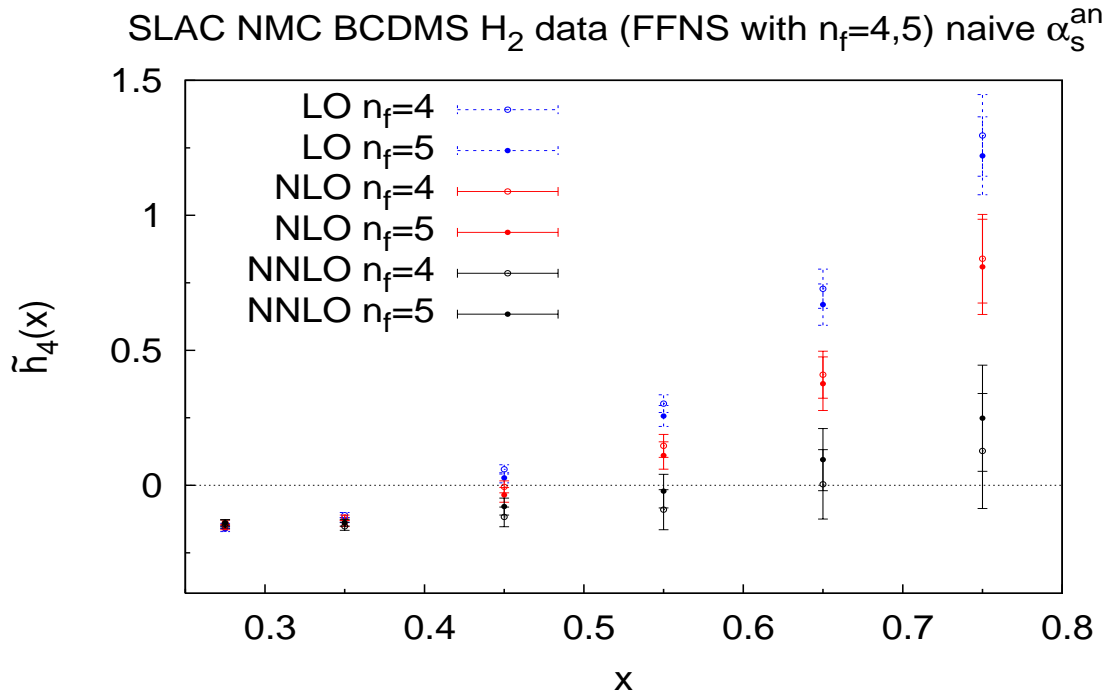


Figure 5: Comparison of the HTC parameter  $\tilde{h}_4(x)$  obtained in LO, NLO and NNLO for hydrogen data within a FFNS between the cases with  $n_f = 4$  and  $n_f = 5$  and the naive analytic  $\alpha_s$ .

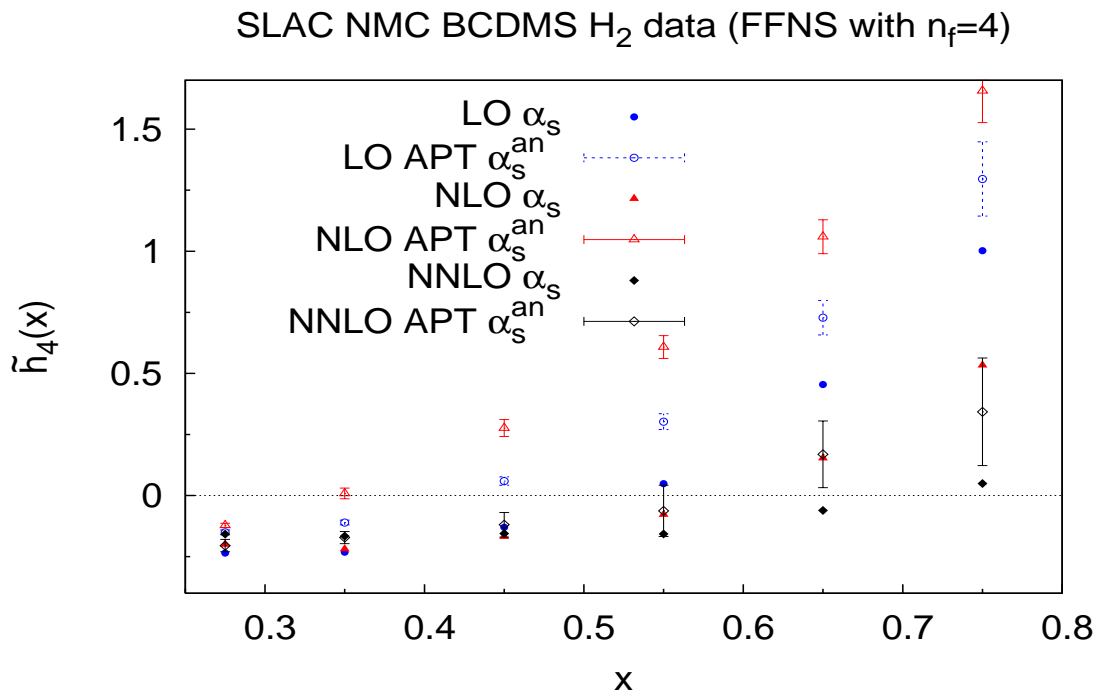


Figure 6: Comparison of the HTC parameter  $\tilde{h}_4(x)$  obtained in LO, NLO and NNLO for hydrogen data within a FFNS ( $n_f = 4$ ) between the cases with a standard perturbative and APT-inspired  $\alpha_s$ .

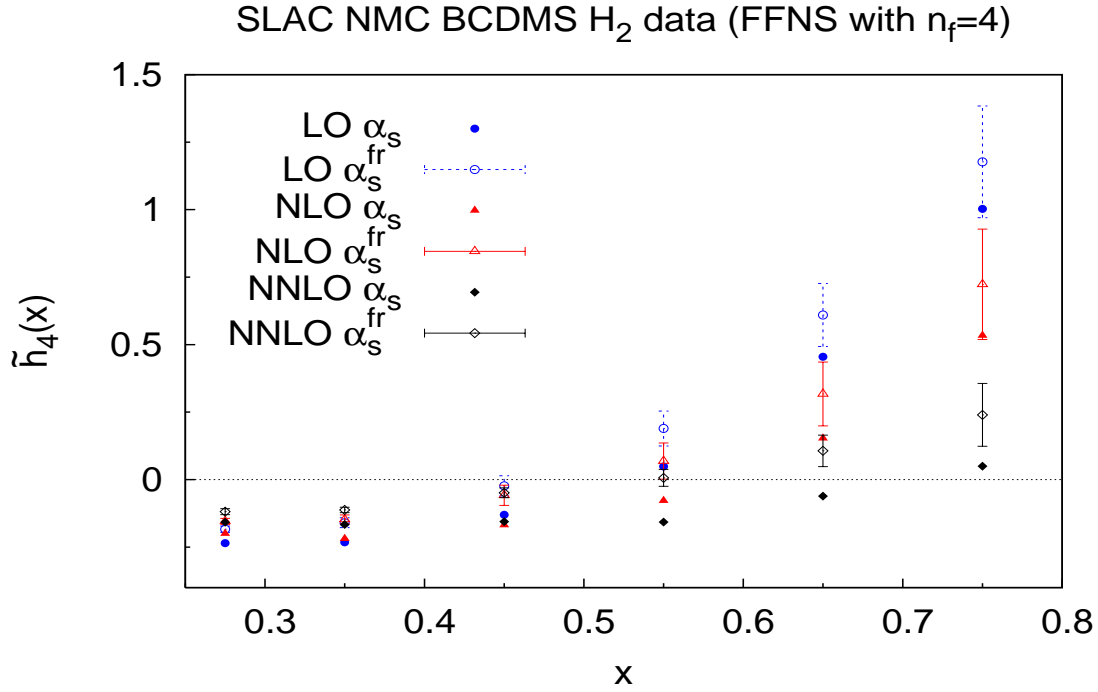


Figure 7: Comparison of the HTC parameter  $\tilde{h}_4(x)$  obtained at LO, NLO and NNLO for hydrogen data within a FFNS ( $n_f = 4$ ) between the cases with a standard perturbative and “frozen”  $\alpha_s$ .

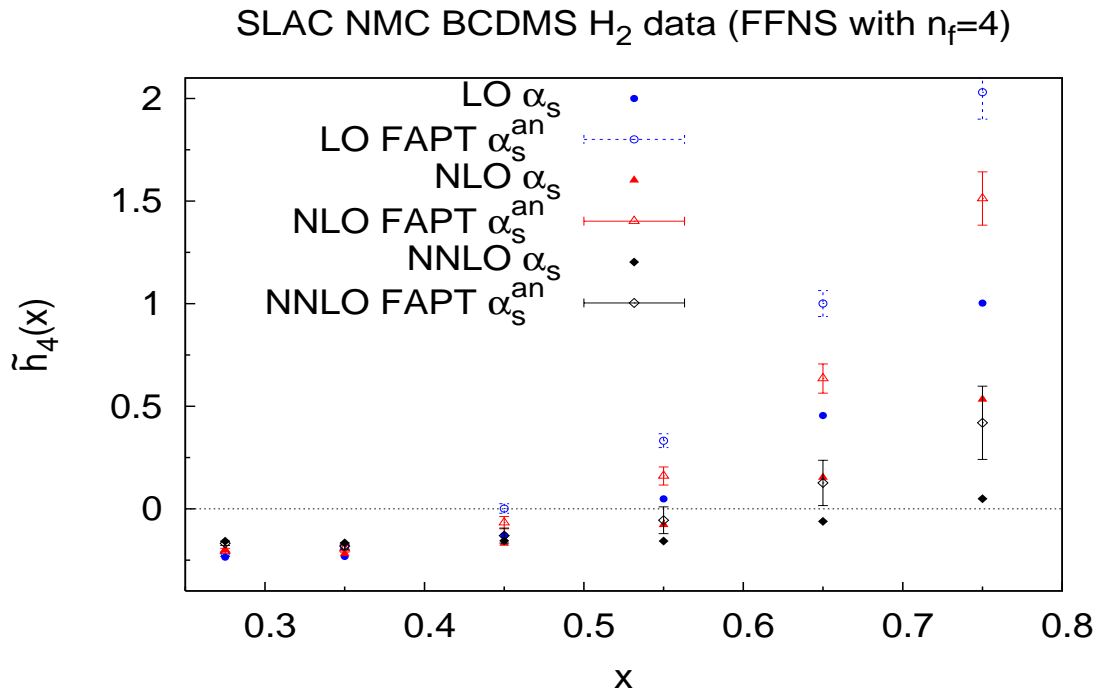


Figure 8: Comparison of the HTC parameter  $\tilde{h}_4(x)$  obtained at LO, NLO and NNLO for hydrogen data within a FFNS ( $n_f = 4$ ) between the cases with a standard perturbative and FAPT-inspired  $\alpha_s$ .